Journal of Nuclear Materials 401 (2010) 154–158

Contents lists available at ScienceDirect

Journal of Nuclear Materials

journal homepage: www.elsevier.com/locate/jnucmat

Phase-field simulation of nucleation and growth of $M_{23}C_6$ carbide and ferromagnetic phases during creep deformation in Type 304 steel

Yuhki Tsukada [a,*], Atsuhiro Shiraki [a,1], Yoshinori Murata [a], Shigeru Takaya [b], Toshiyuki Koyama [c], Masahiko Morinaga [a]

[a] Department of Materials, Physics and Energy Engineering, Graduate School of Engineering, Nagoya University, Furo-cho, Chikusa-ku, Nagoya 464-8603, Japan
[b] Japan Atomic Energy Agency, 4002 Narita-cho, O-arai-machi, Higashi-ibaraki-gun, Ibaraki 311-1393, Japan
[c] National Institute for Materials Science, 1-2-1 Sengen, Tsukuba, Ibaraki 305-0047, Japan

ARTICLE INFO

Article history:
Received 16 December 2009
Accepted 9 April 2010

ABSTRACT

A phase-field method was applied to the simulation of simultaneous nucleation and growth of both $M_{23}C_6$ carbide and ferromagnetic α phases during the creep process in Type 304 steel. Nucleation events of these product phases were explicitly introduced through a probabilistic Poisson seeding process based on local nucleation rates that were calculated as a function of local concentration. The defect energy of the creep dislocations near the carbides, which increases during creep, was integrated into the nucleation driving force for the α phase. The simulation used in this study accurately reproduced changes in the amounts of the precipitated phases as a function of creep time. Furthermore, we examine the effect of the dislocation density on precipitation of the α phase, and show that the phase-field method is useful for examining the stochastic and kinetic phenomenon of phase transformation.

1. Introduction

Type 304 austenitic steel is a high temperature material that is used for structural elements of nuclear power plants. It has been reported that (a) its magnetic properties change during creep tests at high temperatures because of the formation of a ferromagnetic phase, especially near $M_{23}C_6$ carbide [1,2], (b) a significant proportion of creep dislocations are trapped in creep process by the carbide, and (c) the dislocation density is high near the carbide [3]. Furthermore, it has been shown that the creep dislocation energy may be the main driving force for nucleation of the ferromagnetic α phase, which is calculated as an equilibrium phase at high temperatures based on the thermodynamic database [3]. From these phenomena, it is important to correlate the defect energy of the creep dislocations with changes in the amount of the ferromagnetic phase because it may be possible to develop a non-destructive evaluation technique to estimate creep damage in the steel by detecting changes in its magnetic properties.

In recent years, the phase-field method has been applied to simulate phase transformations and microstructural evolutions in materials. This approach allows the simultaneous simulation of nucleation and growth processes, by seeding nuclei stochastically in an evolving microstructure at a nucleation rate that is calculated on the basis of the classical nucleation theory, as a function of both local concentration and temperature [4–7]. In this theory, the driving force for nucleation is the reduction in the bulk free energy upon the formation of a unit volume of a product phase from a matrix, and it is possible to incorporate the creep dislocation energy into a part of the nucleation driving force for the ferromagnetic α phase in Type 304 steel if the local dislocation energy density in the material can be estimated.

The purpose of this study is to examine the effect of creep dislocation energy on the change in the amount of the α phase generated in Type 304 steel using the phase-field method. The distribution function of the local creep dislocations near the $M_{23}C_6$ carbide is calculated on the basis of a previously reported experiment [3]. Concurrent nucleation and growth of the carbide phase and the α phase as the ferromagnetic phase are simulated by a model that treats the dislocation energy as a part of the nucleation driving force for the α phase. Changes in the relative amounts of these two product phases, during the creep process in Type 304 steel, are first reproduced using the phase-field method, and then the correlation of the dislocation density with the phase transformation is examined.

2. Calculation method

2.1. Phase-field model

To simulate phase transformation in Type 304 steel, we consider the concentrations of basic constituent elements, $c_x(\mathbf{r}, t)$,

* Corresponding author. Tel.: +81 52 789 5342; fax: +81 52 789 3232.
E-mail address: tsukada@silky.numse.nagoya-u.ac.jp (Y. Tsukada).
[1] Present address: Kobe Steel, Ltd., 2222-1 Onoecho Ikeda, Kakogawa, Hyogo 675-0023, Japan.

0022-3115/$ - see front matter © 2010 Elsevier B.V. All rights reserved.
doi:10.1016/j.jnucmat.2010.04.017

(x = Fe, Cr, Ni, C), which vary spatially ($\mathbf{r}$) and temporally (t). In this study, the average composition is Fe – 18.59 mass% Cr – 8.92% Ni – 0.05% C, and the volume fractions of equilibrium phases of the system at 873 K ($f_i(\mathbf{r},t)$, i = γ, α, $M_{23}C_6$) are employed as field variables and are calculated using the thermo-calc Ver. FE-6 thermodynamic database (hereinafter referred to as the thermo-calc database). This model is suitable to be applied in practical multi-component systems because $f_i(\mathbf{r},t)$ is selected as the field variable instead of $c_x(\mathbf{r},t)$. The concentration fields are then given as

$$c_x(\mathbf{r},t) = \sum_i f_i(\mathbf{r},t) c_x^{i:eq}, \tag{1}$$

where $c_x^{i:eq}$ is the equilibrium concentration of element x in phase i and is calculated using the thermo-calc database. The temporal evolution of the field variables are given by the Cahn–Hilliard equations

$$\frac{\partial f_i(\mathbf{r},t)}{\partial t} = M_i \nabla^2 \frac{\delta G_{sys}}{\delta f_i(\mathbf{r},t)}, \tag{2}$$

where M_i is the interfacial mobility and G_{sys} is the total free energy of the system, which is given by

$$G_{sys} = \int_{\mathbf{r}} \left[G_{chem}(\mathbf{r},t) + E_{grad}(\mathbf{r},t) \right] d\mathbf{r}, \tag{3}$$

where G_{chem} is the chemical free energy density and E_{grad} is the gradient energy density. The chemical free energy density is expressed as

$$G_{chem} = \{1 - h(f_\alpha) - h(f_{M_{23}C_6})\} G_{chem}^{\gamma}(c_x) + h(f_\alpha) G_{chem}^{\alpha}(c_x) + h(f_{M_{23}C_6}) G_{chem}^{M_{23}C_6}(c_x) + w \sum_{i \neq j} f_i f_j, \tag{4}$$

where w is the height of the energy barrier between phases i and j, and $G_{chem}^{i}(c_x)$ is the chemical free energy density of phase i. At constant temperature, $G_{chem}^{i}(c_x)$ is formulated as a function of concentrations and can be calculated using the thermo-calc database. The function $h(f_i)$ is

$$h(f_i) = f_i^3 (10 - 15 f_i + 6 f_i^2). \tag{5}$$

The gradient energy density is evaluated from the field variables using

$$E_{grad} = \frac{1}{2} \sum_i \kappa_i (\nabla f_i)^2, \tag{6}$$

where κ_i is the gradient energy coefficient [8].

2.2. Description of a nucleation event

A product phase nucleation event is incorporated by seeding nuclei in an evolving microstructure according to nucleation rates calculated on the basis of classical nucleation theory [4–7]. The steady-state nucleation rate for a thermally activated process is

$$J_i = J_0 \exp(-\Delta G_i / k_B T), \tag{7}$$

where J_0 is the pre-exponential factor, k_B is the Boltzmann constant, and T is the absolute temperature. On the basis of the nucleation rate calculated by Eq. (7), nucleation events are explicitly introduced through a probabilistic Poisson seeding process. The quantity ΔG_i is the activation energy for nucleation and is estimated by considering an isolated sphere of product phase embedded in an infinite homogeneous supersaturated matrix phase. In the two-dimensional simulation, the activation energy is

$$\Delta G_i = \frac{\pi \gamma_i^2}{\Delta f_i}, \tag{8}$$

where γ_i is the interfacial energy and Δf_i is the bulk driving force for nucleation. In this study, we consider the nucleation of $M_{23}C_6$ carbide and α phase with equilibrium phase compositions from the supersaturated γ phase, and we calculate Δf_i using the thermo-calc database as

$$\Delta f_\alpha = G_{chem}^{\gamma}(c_x) - G_{chem}^{\alpha}(c_x^{\alpha:eq}) + \sum_x \frac{\partial G_{chem}^{\gamma}}{\partial c_x} (c_x^{\alpha:eq} - c_x) + E_d, \tag{9}$$

$$\Delta f_{M_{23}C_6} = G_{chem}^{\gamma}(c_x) - G_{chem}^{M_{23}C_6}(c_x^{M_{23}C_6:eq}) + \sum_x \frac{\partial G_{chem}^{\gamma}}{\partial c_x} (c_x^{M_{23}C_6:eq} - c_x). \tag{10}$$

In Eqs. (9) and (10), c_x is a function of the spatial position ($\mathbf{r}$), so Δf_i represents the local driving force for nucleation. Furthermore, because the creep dislocation energy can be a part of the nucleation driving force for the α phase [3], the dislocation energy density (E_d) is introduced into Δf_α as shown in Eq. (9). The dislocation energy density is approximated using

$$E_d = \left[\frac{\mu b^2}{4\pi} \ln\left(\frac{r}{r_0}\right) \right] \cdot \rho(\mathbf{r},t), \tag{11}$$

where μ is the shear modulus, b is the magnitude of the Burgers vector, r_0 is the cutoff radius of the dislocation core, r is the outer cutoff radius, and ρ is the local dislocation density. In this study, we use $r_0 = 5b$ and $r = b \times 10^4$ [9]. On the basis of the experimental fact that the dislocation density is high near $M_{23}C_6$ carbide during the creep process [3], the local dislocation density ρ is defined as

$$\rho(\mathbf{r},t) = \rho_0(t) \exp(-B \cdot |\mathbf{r} - \mathbf{r}'|), \tag{12}$$

and

$$\rho_0(t) = a_1 \cdot (t/t_r)^{1/5} + a_2, \tag{13}$$

where $\rho_0(t)$ is the dislocation density at the interface between the carbide and the matrix, t is the creep time, t_r is the time to rupture, and $\mathbf{r}'$ is the position of the interface. In Eqs. (12) and (13), B, a_1, and a_2 are coefficients that depend on the applied stress and temperature.

The conventional difference method is employed to numerically solve Eq. (2). The physical parameters are reduced to dimensionless quantities using the scaling factor of RT for the energy scale and λ for length scale, where R is the gas constant, T is the absolute temperature, and λ is the unit grid size. The time scale is reduced to dimensionless time using $t^* = t \times (10 M_i RT/\lambda^2)$, where the asterisk denotes a dimensionless quantity.

2.3. Simulation conditions

We perform a two-dimensional phase-field simulation at 873 K under periodic boundary conditions. The system size is 256 × 256 nm^2 with a unit grid size of λ = 2 nm, and a molar volume $V_m = 6.92 \times 10^{-6} m^3/mol$ is used for the entire system. The parameters in the simulation are $w = 1.43 \times 10^7$ J m^{-3}, $\kappa_i = 7.18 \times 10^{-9}$ J m^{-1}, μ = 77.4 GPa [10], b = 0.255 nm [11], and $\Delta t^* = 0.003$. The interfacial energy of each phase is $\gamma_{M_{23}C_6} = 0.5$ J m^{-2} and $\gamma_\alpha = \gamma_{M_{23}C_6}/A$, respectively, where A is a fitting parameter. The pre-exponential factor in Eq. (7) is $J_0^* = 2.2 \times 10^{51}$. The coefficients in Eqs. (12) and (13) are $B = 2.54 \times 10^7$ m^{-1}, $a_1 = 1.40 \times 10^{15}$ m^{-2}, and $a_2 = 1.71 \times 10^{13}$ m^{-2}, which are determined using the experimental data of the dislocation density near the carbide during creep at 873 K under 172 MPa, where the time to rupture is t_r = 780 h [3]. In the simulation, the time to rupture t_r, and the parameter A, are set to be t^* = 45 and A = 5.24, respectively, so as to reproduce the experimental results for the changes in the amounts of product phases.

Fig. 1 shows the distribution function of the dislocation density near $M_{23}C_6$ carbide as a function of distance from the carbide interface ($l = |\mathbf{r} - \mathbf{r}'|$) at $t/t_r = 0.01$, $t/t_r = 0.05$, and $t/t_r = 0.20$. As shown in Fig. 1, Eq. (12) is chosen to reproduce

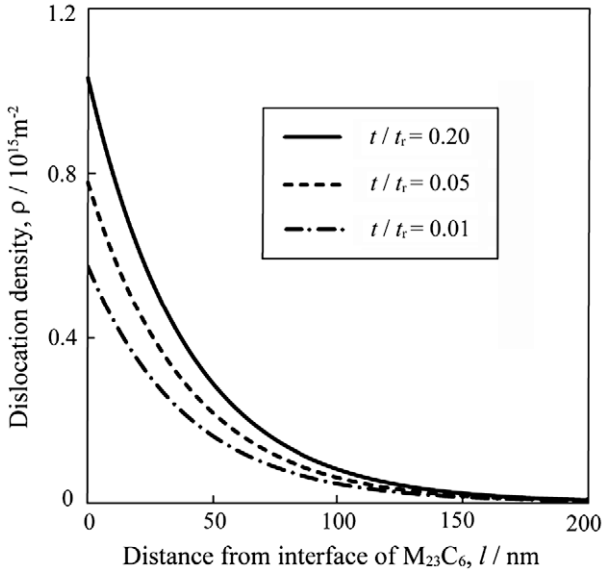

Fig. 1. Distribution of dislocation density near $M_{23}C_6$ carbide at $t/t_r = 0.01$, $t/t_r = 0.05$, and $t/t_r = 0.20$ as a function of distance from the carbide interface. The quantity t_r is the time to rupture in the creep test.

the high dislocation density near the carbide. Fig. 2 shows the increase in the dislocation density with creep time normalized by the time to rupture (t_r). In Fig. 2, the solid line corresponds to $a_1 = 1.40 \times 10^{15}\ m^{-2}$.

In considering the distribution of the dislocation density in the simulation, it is computationally difficult to determine the distance from the interface of the precipitated carbide at every time step. Based on the reported size of the carbide [3], it can be said that for efficient computation, the position of the interface needs to be set to seven grid steps from the spot, where the carbide nucleation event occurred in the simulation.

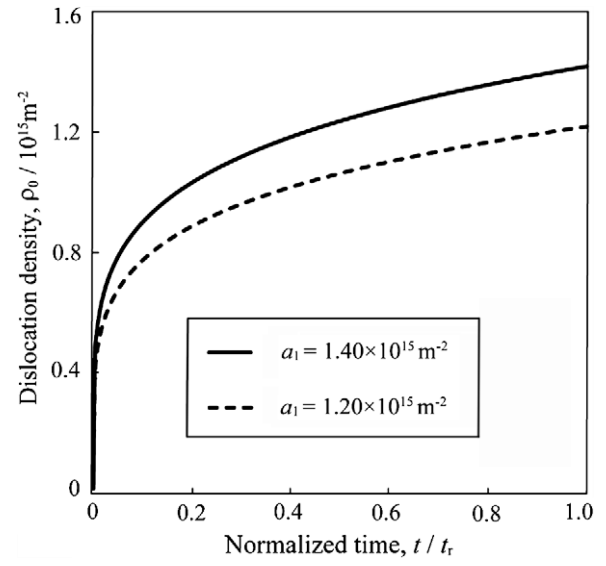

Fig. 2. Change in dislocation density at the interface of $M_{23}C_6$ carbide with the creep time normalized by the time to rupture (t_r). The quantity a_1 is a coefficient in the distribution function of the dislocation density.

3. Simulation results

3.1. Changes in the mole fraction of product phase generated

Fig. 3 shows the results obtained from two-dimensional phase-field simulation at 873 K. In Fig. 3, the white and gray areas correspond to $M_{23}C_6$ carbide phase and α phase, respectively, and the results for different time steps are shown: (a) $t^* = 6$, (b) $t^* = 12$, (c) $t^* = 15$, (d) $t^* = 18$, (e) $t^* = 21$, (f) $t^* = 24$, (g) $t^* = 27$ and (h) $t^* = 45$, where t^* represents the dimensionless time step. The nucleation of the carbide occurs instantaneously at the initial stage of the simulation, and the precipitated carbide coarsens with simulation time. However, the nucleation of the ferromagnetic α phase first occurs around $t^* = 9$–12. Coarsening of the α phase is scarcely observed, and the increase in the amount of the α phase primarily originates from the subsequent precipitation near the carbides.

Changes in the mole fractions of the $M_{23}C_6$ carbide phase and the α phase as a function of simulation time are shown in Figs. 4 and 5, respectively. From Fig. 4, we see that the amount of carbide gradually increases up to a mole fraction of 0.0077 at $t^* = 45$. This result is consistent with the experimental result that the mole fraction of the carbide phase reaches 0.0073 at $t/t_r = 1$ [3]. In Fig. 5, closed circles represent the result with $a_1 = 1.40 \times 10^{15}\ m^{-2}$, and we see that the mole fraction of the α phase increases after the first nucleation and saturates around $t^* = 27$. Thus, the simulation reproduces the experimental fact that the increase in the ferromagnetic phase is scarcely observed in the late stage of creep [2].

3.2. Effect of dislocation density on the precipitation behavior of the α phase

The simulation reproduces the experimental results regarding changes in the relative amount of generated product phase. To clarify the effect of the dislocation density on the precipitation behavior of the α phase, the coefficient in Eq. (13) is changed to $a_1 = 1.20 \times 10^{15}\ m^{-2}$, and the other parameters are set to the same values as used in Section 3.1. This condition corresponds to the case, where the dislocation density near the carbide is relatively low during the creep process, as shown by the dashed line in Fig. 2. The resulting change in the mole fraction of the α phase given by the simulation is shown by the open circles in Fig. 5. We find that the beginning of the nucleation of the α phase is delayed until $t^* = 15$–18. Furthermore, the saturation time of the precipitation is also delayed until $t^* = 36$. Thus, a small difference in the dislocation density leads to a significant difference in the saturation time.

4. Discussion

With regard to the changes in the mole fraction of product phase generated, the experimental results were reproduced by the simulation, as shown in Section 3.1. Here, the change in the mole fraction of carbide phase generated was consistent with the result of extraction residue analysis reported previously [3]. As for the amount of α phase generated, it was qualitatively reproduced in the sense that it started to increase in the initial stage of creep and saturated in the later stages of creep [2]. However, the saturation amount of the α phase has not been quantitatively revealed. If the saturation amount in the creep process of the practical steel is examined quantitatively in future research, quantitative simulations of both the phase transformations and the changes in the mole fraction of the product phase generated would be possible.

On the basis of the simulation presented in Section 3.1, we examine the effect of the dislocation energy on the precipitation

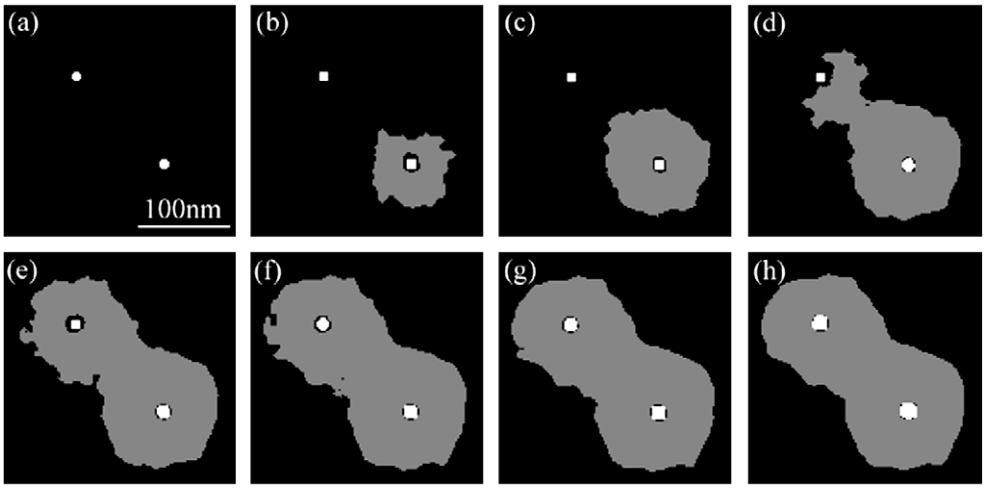

Fig. 3. Results of two-dimensional phase-field simulation at 873 K: (a) $t^* = 6$, (b) $t^* = 12$, (c) $t^* = 15$, (d) $t^* = 18$, (e) $t^* = 21$, (f) $t^* = 24$, (g) $t^* = 27$, and (h) $t^* = 45$, where t^* is the dimensionless time step. The white and gray areas represent the $M_{23}C_6$ carbide phase and the α phase, respectively.

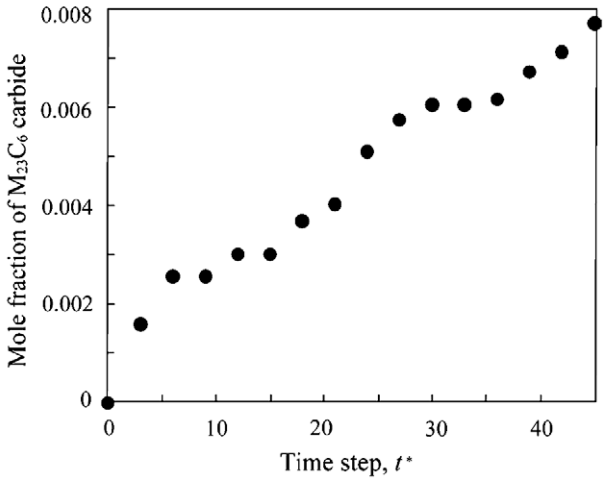

Fig. 4. Change in mole fraction of $M_{23}C_6$ carbide with time step in the phase-field simulation.

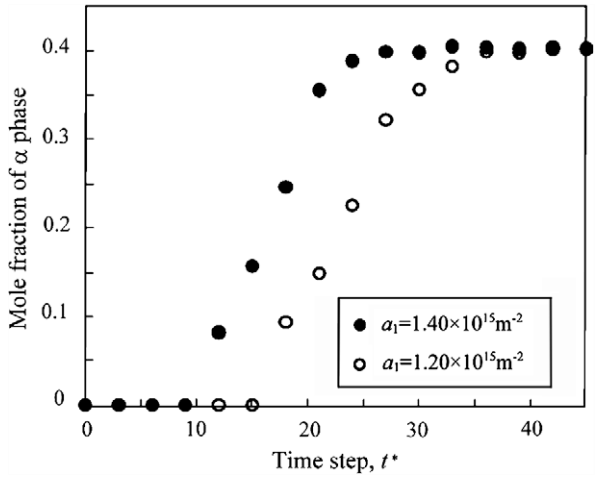

Fig. 5. Change in mole fraction of the α phase with time step in the phase-field simulation. The quantity a_1 is a coefficient in the distribution function of the dislocation density.

behavior of the α phase in this system, as shown in Section 3.2. We confirm that this model can examine the stochastic phenomenon that the decrease in the dislocation density near the carbide leads to the delay in the saturation time of the precipitation of the α phase. To correlate the defect energy during creep deformation with the mole fraction of α phase in various stress conditions, the change in the dislocation density near the carbide in creep process should be assessed quantitatively as a function of the applied stress. When the dislocation density is estimated, it is desirable to use the phase-field method we propose in this study to confirm whether or not the change in the magnetic properties would occur under service stress conditions. We expect that the phase-field method can become one of the tools used to develop a non-destructive evaluation technique.

The simulation in this paper focuses on the changes in the mole fraction of product phase generated, so it fails to describe the morphological changes in the product phases. For example, it has been reported that, in the coarsening process, $M_{23}C_6$ carbide assumes energetically favorable shapes such as rectangular, square, or rhombic [12]. If the formation mechanism of such characteristic shapes is revealed, it might be possible to reproduce the morphological change by incorporating the anisotropic coherent energy or the anisotropic interfacial energy into the model. The same thing can be said about the α phase, whose precipitation morphology during the creep process has not been reported yet.

With regard to the description of the nucleation process, there have been some reports, where the strain energy of nucleus formation; i.e., the precipitation energy of coherent particles, was incorporated into the phase-field model to consider the effect of elastic interaction on nucleation [6,7]. In the present study, the strain energy is ignored for simplicity, except that the self-elastic energy of the creep dislocations is incorporated into a part of the nucleation driving force for the α phase. In future research, it is expected that the present model will be extended to a simulation study with larger length scales, which includes grain boundaries that can also serve as nucleation sites for the product phases.

5. Conclusions

We perform a phase-field simulation on concurrent nucleation and growth of both the $M_{23}C_6$ carbide phase and the ferromagnetic α phase during the creep process in Type 304 steel. The local nucleation driving force for the product phases was calculated as a function of the local concentrations that were derived using classical

nucleation theory. Furthermore, the creep dislocation energy near the carbides was integrated into the nucleation driving force for the α phase. The simulated results for the mole fractions of the product phases are consistent with previously reported experimental results. We find that the precipitation behavior of the α phase is correlated with the dislocation density during the creep process. This fact indicates that the model is useful to examine the stochastic and kinetic phenomenon of the phase transformation.

Acknowledgements

This work was supported by a Grant-in-Aid for JSPS Fellows of the Ministry of Education, Culture, Sports, Science and Technology, Japan, and was also supported in part by a Grant-in-Aid for Scientific Research of Japan Society for the Promotion of Science (JSPS), Japan.

References

[1] Y. Nagae, Mater. Sci. Eng. A 387–389 (2004) 665–669.
[2] Y. Nagae, K. Aoto, J. Soc. Mater. Sci., Japan 54 (2005) 116–121.
[3] Y. Tsukada, A. Shiraki, Y. Murata, S. Takaya, T. Koyama, M. Morinaga, J. Nucl. Mater. in press, doi:10.1016/j.jnucmat.2010.03.013.
[4] J.P. Simmons, C. Shen, Y. Wang, Sci. Mater. 43 (2000) 935–942.
[5] J.P. Simmons, Y. Wen, C. Shen, Y.Z. Wang, Mater. Sci. Eng. A 365 (2004) 136–143.
[6] C. Shen, J.P. Simmons, Y. Wang, Acta Mater. 54 (2006) 5617–5630.
[7] C. Shen, J.P. Simmons, Y. Wang, Acta Mater. 55 (2007) 1457–1466.
[8] J.W. Cahn, J.E. Hilliard, J. Chem. Phys. 28 (1958) 258–267.
[9] M. Kato, Introduction to the Theory of Dislocations, Shokabo, Tokyo, 1999.
[10] H.M. Ledbetter, J. Appl. Phys. 52 (1981) 1587–1589.
[11] A. Boeuf, S. Crico, R. Caciuffo, F. Rustichelli, I. Pomot, G. Uny, Mater. Lett. 3 (1985) 115–118.
[12] F.R. Beckitt, B.R. Clark, Acta Metall. 15 (1967) 113–129.